Phosphorylation of Galectin-3 Contributes to Malignant Transformation of Human Epithelial Cells via Modulation of Unique Sets of Genes

Nachman Mazurek,[1] Yun Jie Sun,[1] Janet E. Price,[2] Latha Ramdas,[3] Wendy Schober,[4] Pratima Nangia-Makker,[5] James C. Byrd,[1] Avraham Raz,[5] and Robert S. Bresalier[1]

Departments of [1]Gastrointestinal Medicine and Nutrition, [2]Cancer Biology, [3]Experimental Radiation Oncology, and [4]Blood and Marrow Transplantation, The University of Texas M.D. Anderson Cancer Center, Houston, Texas and [5]The Tumor Progression and Metastasis Program, Karmanos Cancer Institute, Wayne State University, Detroit, Michigan

Abstract

Galectin-3 is a multifunctional β-galactoside-binding protein implicated in apoptosis, malignant transformation, and tumor progression. The mechanisms by which galectin-3 contributes to malignant progression are not fully understood. In this study, we found that the introduction of wild-type galectin-3 into nontumorigenic, galectin-3-null BT549 human breast epithelial cells conferred tumorigenicity and metastatic potential in nude mice, and that galectin-3 expressed by the cells was phosphorylated. In contrast, BT549 cells expressing galectin-3 incapable of being phosphorylated (Ser^6→Glu Ser^6→Ala) were nontumorigenic. A microarray analysis of 10,000 human genes, comparing BT549 transfectants expressing wild-type and those expressing phosphomutant galectin-3, identified 188 genes that were differentially expressed (>2.5-fold). Genes affected by introduction of wild-type phosphorylated but not phosphomutant galectin-3 included those involved in oxidative stress, a novel noncaspase lysosomal apoptotic pathway, cell cycle regulation, transcriptional activation, cytoskeleton remodeling, cell adhesion, and tumor invasion. The reliability of the microarray data was validated by real-time reverse transcription-PCR (RT-PCR) and by Western blot analysis, and clinical relevance was evaluated by real-time RT-PCR screening of a panel of matched pairs of breast tumors. Differentially regulated genes in breast cancers that are also predicted to be associated with phospho-galectin-3 in transformed BT549 cells include C-type lectin 2, insulin-like growth factor-binding protein 5, cathepsins L2, and cyclin D1. These data show the functional diversity of galectin-3 and suggest that phosphorylation of the protein is necessary for regulation (directly or indirectly) of unique sets of genes that play a role in malignant transformation. (Cancer Res 2005; 65(23): 10767-75)

Introduction

Galectins are a family of carbohydrate-binding proteins that have been well conserved through evolution and are abundant in epithelial and immune cells of animals (1, 2). These proteins have sequence similarities in the carbohydrate recognition domain and specificity for β-galactoside moieties found on both N- and O-linked glycans (3, 4). To date, 14 members of the galectin family have been identified and classified into proto, chimera, and tandem-repeat types according to their structure (5). Galectin-3 is a 31 kDa chimeric gene product consisting of three distinct structural domains: a short NH_2-terminal domain of 12 amino acids, which controls its cellular targeting; a repetitive collagen-like sequence rich in glycine, tyrosine, and proline, which serves as a substrate for matrix metalloproteinases; and a carboxy-terminal domain with a globular structure encompassing the carbohydrate-binding site (6–8).

Galectin-3 has pleiotropic biological functions depending on its subcellular location. Extracellular galectin-3 mediates cell migration, cell adhesion, and cell-to-cell interactions (8), whereas intracellular galectin-3 inhibits apoptosis (9–11) and is up-regulated during neoplastic progression and metastasis in several human malignancies, including cancers of the thyroid, colon, liver, and brain (12–16). Furthermore, wild-type galectin-3 is capable of malignant transformation of thyroid follicular cells and human breast epithelial cells (17, 18). Galectin-3 is also found in the nucleus as a nuclear matrix protein involved in pre-mRNA splicing (19) and may regulate gene expression (e.g., cyclin D_1 and MUC2) through the activation of specific transcription factors [e.g., activator protein1 (AP-1), nuclear factor of activated T cell (NFAT), SP1, cyclic AMP (cAMP)–responsive element binding protein, and thyroid transcription factor-1; refs. 20–23].

Galectin-3 undergoes phosphorylation at Ser^6 by casein kinase 1 and dephosphorylation by protein phosphatase 1 (24, 25). This posttranslational modification signaling acts as an "on/off" switch for its carbohydrate-binding capability (25). Recent studies have shown that phosphorylation of nuclear galectin-3 at Ser^6 is critical for its transport from the nucleus and for its antiapoptotic functions (26, 27). Here, we present evidence that phosphorylation of galectin-3 also plays a key role in malignant transformation and is associated with the activation of specific sets of genes and pathways. This work provides new insights into the molecular mechanisms underlying the role of galectin-3 in tumorigenesis and metastasis.

Materials and Methods

Cell lines and culture conditions. Parental BT549 cells were obtained from Dr. E.W. Thompson. The establishment of a stable neoresistant control vector-transfected BT549 clone (BT549V), two wild-type galectin-3-transfected BT549 clones (BT549 gal 25A and BT549 gal 25B), and four phosphomutant galectin-3 BT549 transfectant clones (BT549SE51, BT549SE56, BT549SA7, and BT549SA9) was previously described (7, 26, 27). Phosphomutant galectin-3 was generated by substitution of the Ser^6 residue

Note: Supplementary data for this article are available at Cancer Research Online (http://cancerres.aacrjournals.org/).

Requests for reprints: Robert S. Bresalier, Department of Gastrointestinal Medicine and Nutrition, The University of Texas M.D. Anderson Cancer Center, Unit 436, 1515 Holcombe Boulevard, Houston, TX 77030. Phone: 713-745-4340; Fax: 713-745-9295; E-mail: rbresali@mdanderson.org.

doi:10.1158/0008-5472.CAN-04-3333

by glutamic acid (SE clones) or alanine (SA clones) using a Quick Change site-directed mutagenesis kit (Stratagene, La Jolla, CA) as described previously (7, 26, 27). BT549 cells were cultured in RPMI 1640 supplemented with 10% heat-inactivated fetal bovine serum, L-glutamine (2 mmol/L), penicillin (100 units/mL), and streptomycin (50 units/mL) in a 95% air and 5% CO_2 incubator at 37°C. The stable transfected clones were maintained in complete RPMI 1640 containing the antibiotic G418 (200 μg/mL).

Mice. Female athymic NCr-nu mice were purchased from the National Cancer Institute-Frederick Cancer Research Facility (Frederick, MD). The mice were housed in the approved specific pathogen-free facility of our institution and used at 7 to 8 weeks of age. The care and use of laboratory animals was approved by The University of Texas M.D. Anderson Cancer Center Institutional Animal Care and Use Committee.

Immunofluorescence staining and flow cytometry. Cells were fixed, permeabilized, and blocked in flow cytometry buffers (Santa Cruz Biotechnology, Santa Cruz, CA) following the instructions of the manufacturer. Cells were double stained with a 1:100 dilution of rat anti-galectin-3 monoclonal antibody (TIB166, 0.26 mg/mL; American Type Culture Collection, Manassas, VA) and a 1:500 dilution of rabbit anti-phospho galectin-3 (Ser^6, 0.88 mg/mL) for 1 hour at room temperature. Anti-phosphogalectin-3 antibody was established in conjunction with Zymed Laboratories (South San Francisco, CA) by immunizing rabbits against a synthetic phosphopeptide comprising of 14 NH_2-terminal amino acids of galectin-3 phosphorylated at Ser^6 [DNF (pS) LHDALSGSGN (C)]. The antibody was affinity purified on an immobilized "hot" peptide followed by affinity absorption on an immobilized "cold" peptide. The specificity of the antibody was determined by a differential ELISA using hot and cold peptides. Western blot analysis of human recombinant galectin-3 and a phosphorylated protein also confirmed specificity of the antibody for phosphorylated galectin-3. Secondary antibodies, FITC-conjugated goat anti-rat (Chemicon, Temecula, CA), and phycoerythrin-conjugated goat anti-rabbit (Molecular Probes, Eugene, OR) were added at 1:200 dilution and incubated for 30 minutes at room temperature. In each experiment, 10^6 cells were processed for flow cytometric analysis on a FACSCalibur apparatus (Becton Dickinson, Franklin Lakes, NJ). The dual labeling was analyzed by Cell Quest PRO software (Becton Dickinson). Single color–stained cells were used for instrument compensation.

Protein extraction and Western blot analysis. Total cell lysate extractions and Western blots were done as previously described (25). The blots were then probed with anti-galectin-3 or anti-cyclin D1 (Calbiochem, La Jolla, CA); anti-MUC2, anti-MUC5AC, or anti-MUC1 (Vector Laboratories, Burlingame, CA); anti–insulin-like growth factor binding protein 5 (IGFBP5), anti-PRSS3, anti–dual specificity phosphatase 6 (DUSP6), and anti-CTSL2 (Santa Cruz Biotechnology): or anti-β-actin (Sigma, St. Louis, MO) as a controls for loading in each lane, followed by the appropriate horseradish peroxidase–conjugated secondary antibodies (Chemicon). The antigen was detected using the enhanced chemiluminescence detection system (Amersham, Piscataway, NJ) according to the instructions of the manufacturer.

Tumorigenicity assay. Cells were harvested from cultures of BT549/V, BT549 gal 25A, BT549 gal 25B, BT549SE51, BT549SE56, BT549SA7, and BT549SA9 using 0.02% EDTA and resuspended in Ca^{2+}- and Mg^{2+}-free PBS. Nude mice were injected with 2×10^6 cells mixed in 0.1 mL Matrigel (Becton Dickinson) into the mammary fat pad as described previously (28). Tumor diameters were measured weekly using calipers. Results were pooled from two separate experiments and all experiments were done with the approval of the Institutional Animal Core and Ethics Committee. Statistical analysis was done using StatView 4.02. All tests were two sided, with $P = 0.05$ regarded as significant.

Spontaneous lung micrometastasis assay. BT549 transfectant cells (1×10^6) mixed with 2 mL of Matrigel were injected into the mammary fat pad of 6 to 8-week-old immunodeficient nude mice (NCR-NV, Taconic Farms, Germantown, NY). Mice were sacrificed by CO_2 inhalation 4 to 5 weeks after injection. At autopsy, the lungs were removed and examined for micrometastases. The lungs were washed with Hank's buffer, minced, and incubated with 5 mL DMEM containing 5 mg collagenase type IV and 36 units elastase on ice for 1 hour. Tissue was placed into a Stomachers bag with fresh medium for 45 seconds. This procedure was repeated twice with fresh medium. Medium were combined and spun at $500 \times g$ for 5 minutes. Cells were resuspended in 2 mL DMEM and plated at different dilutions in the presence of selection medium (800 μg/mL G418). After 1 week, colonies were stained with methylene blue and counted.

Measurement of cell proliferation. BT549 transfectant cell growth *in vitro* was measured using a colorimetric 3-(4,5-dimethylthiazol-2-yl)-5-(3-carboxymethoxyphenyl)-2-(4-sulfophenyl)-2*H*-tetrazolium inner salt (MTS) assay (Promega, Madison, WI). Cells were seeded at 2×10^3 cells per well in 96-well plates and incubated for 24 hours in serum-free medium to synchronize cell growth. Cells were then cultured in 0.1 mL of RPMI 1640 in the presence of 10% FCS. Cell growth was determined at 24-hour intervals by adding 0.02 mL of MTS/phenazine methosulfate solution (Promega). Cells were then incubated at 37°C for 1 hour, and absorbance was determined at 490 nm.

Analysis of cell cycle distribution. Cells were plated at 2×10^5 per well in six-well plates for 2 hours and then incubated in serum-free medium for 48 hours followed by 24-hour incubation in complete medium. Cells were trypsinized and aliquots of 1×10^6 cells were fixed in 70% ethanol at −20°C for 24 hours. Fixed cells were then washed and suspended in 1 mL of fluorochrome solution (PI/RNASE staining buffer, BD Biosciences Clontech, Franklin Lakes, NJ) for 30 minutes in the dark at room temperature. Cell cycle analysis was done using FACSCalibur flow cytometer (BD Biosciences Clontech). Quantitation of cell cycle distribution was done using Mod Fit LT software (Verity Software House, Topsham, ME).

Microarray hybridization. Total RNA was extracted from 80% to 90% confluent BT549/V, BT549 gal 25A, and BT549SE51 clones using Trizol reagent (Invitrogen, Carlsbad, CA) and further purified on RNeasy spin columns (Qiagen, Valencia, CA) according to the manufacturer's directions. Thirty micrograms of total RNA was labeled with Cy3 (BT549/V) or Cy5 (BT549gal 25A and BT549SE51) using the 3DNA Array 350 Expression Array Detection kit (Genisphere, Inc., Hatfield, PA) following the instructions of the manufacturer. The labeled cDNA was purified using a QIAquick PCR Purification kit (Qiagen), dissolved in 40 μL ExpressHyb solution (BD Biosciences Clontech), and heated to 95°C for 10 minutes. The denatured probes were applied to a high-density 10-microarray slide (Unigene), which contains 10,000 randomly spotted oligonucleotides. (Unfortunately, galectin-3 is not included in the microchip gene library of the cancer genomic core laboratory at M.D. Anderson.) Hybridization was done at 60°C for 12 to 16 hours in a humid incubator. After hybridization, the slide was washed at 37°C, once each in 1× SSC, 0.01% SDS, 0.2× SSC, and 0.01% SDS, and then twice in 0.1× SSC. Hybridized arrays were scanned at a 10 μm resolution on a microarray scanner (GeneTaq LSIV; Genomic Solutions, Ann Arbor, MI).

Microarray quantification. Scanned images were quantified in ArrayVision (Imaging Research, Inc., St. Catherine's, Ontario, Canada). Measurements were recorded for spot intensity, local background intensity, and signal-to-noise ratio. Spot intensity was computed as the integrated absorbance or volume in a fixed-size circle. Background intensity was computed as the median pixel value in four diamond-shaped regions at the corners of each spot. The signal-to-noise ratio was computed by dividing the background-corrected intensity by the SD of the background pixels.

Microarray data analysis. Quantified array data were imported into S-Plus software (Insightful Corp., Seattle, WA) for analysis. Background-corrected intensities were globally rescaled to set the 75th percentile in each channel equal to 1,024. Rescaled intensities of <128 were replaced by the threshold value; this threshold was chosen to lie just below the smallest intensity of any spot with a signal-to-noise ratio >1. Next, intensities were transformed by computing the base 2 logarithm. Finally, the log-transformed spot intensities were normalized using robust local regression (29). A spot was identified as differentially expressed if the mean intensity in the two channels exceeded 512 and the estimated change exceeded 2.5-fold or if the mean intensity in the two channels exceeded 256 and the estimated change exceeded 4.5-fold.

Real-time quantitative PCR. Total RNA was isolated from BT549 gal25A, BT549V, BT549SE51, and primary breast tumor specimens as described above. A total of five galectin-3-positive and five grade-matched galectin-3-negative [as determined by real-time quantitative reverse transcription-PCR (RT-PCR)]

invasive ductal carcinomas were obtained from surgical pathology specimens at M.D. Anderson Cancer Center under a protocol approved by the Committee on Human Experimentation and used in this study. Each sample pair was obtained from matched tumor and corresponding normal tissues from the same patient. The BD human reference total RNA is a mixture of total RNAs from multiple adult human tissues chosen to represent a broad range of expressed genes (BD Clontech, Palo Alto, CA). Initial experiments were done to determine the valid range of RNA concentrations and to show the similarity of PCR efficiencies for each gene of interest compared with the endogenous control gene cyclophilin. To determine fold changes in each gene, real-time RT-PCR was done on the ABI Prism 7900 using the commercially available gene expression assay for CCND1, CLECSF2, CTSL2, DUSP6, galectin-3, GFRA1, IGFBP5, and PRSS3 (Hs00277039, Hs00192860, Hs00822401, Hs00169257, Hs00173587, Hs00237133, Hs00181213, and Hs00605637, respectively), and the cyclophilin Vic-labeled Pre-Developed Assay Reagent (Applied Biosystems, Foster City, CA) without multiplexing. A 50 μL final reaction volume containing 1× TaqMan Universal PCR Master Mix without AmpErase UNG (Applied Biosystems), 1× Multiscribe with RNase inhibitors, and 1× gene expression assay was used to amplify 50 ng total RNA with the following cycling conditions: 30 minutes at 48°C, 10 minutes at 95°C, then 50 cycles of 95°C for 15 seconds and 60°C for 1 minute. The 7900 Sequence Detection System 2.2 software automatically determined fold change for each gene in each sample relative to the Becton Dickinson Human Reference Pool using the δδCt method. Calculations were also done for each gene in tumors relative to their corresponding matched normal tissue.

Results

Galectin-3 expression and phosphorylation in stable BT549 transfectants. To assess the role of the phosphorylation of galectin-3 at Ser^6 in malignant transformation, we used BT549 stable transfectants previously established in our laboratory (7, 27) as an experimental cellular model. Parental BT549 cells are nontumorigenic galectin-3-null cells. We transfected these cells with either wild-type galectin-3 (capable of undergoing phosphorylation) or Ser^6 mutants incapable of undergoing phosphorylation (Ser^6→Glu or Ser^6→Ala). After selection with G418, several clones were selected for further analysis: a control clone (BT549/V) expressing a vehicle plasmid, two wild-type galectin-3 clones (BT549gal 25A and gal 25B), two Ser^6→Glu mutant galectin-3 clones (BT549SE51 and SE56), and two Ser^6→Ala mutant galectin-3 clones (BT549SA7 and SA9). Of note is that mutation of human recombinant galectin-3 at Ser^6 did not alter ligand binding but did render it resistant to phosphorylation by casein kinase 1 *in vitro* (25). The expression of galectin-3 in these transfectants was determined by Western blot analysis (Fig. 1*A*) and flow cytometry (Fig. 1*B*). Almost all (>90%) of the cells in the transfectant clones expressed galectin-3 whereas the parental cells and the BT549/V clone control cells did not express detectable levels of galectin-3. The levels of galectin-3 expression varied up to 4-fold between the clones as measured by mean FITC fluorescence intensity (Fig. 1*B*).

A phospho-galectin-3 (Ser^6)–specific antibody was used to monitor the phosphorylation of galectin-3 *in vivo*. Flow cytometric analysis of the BT549 transfectants revealed that 97% of cells transfected with wild-type galectin-3 (gal 25A and gal 25B) expressed high levels of phosphorylated galectin-3, whereas phosphorylated galectin-3 was completely absent in the phosphomutant transfected cells (Fig. 1*B*) The amount of phospho-galectin-3 in gal 25A clone was 1.3-fold higher than in gal 25B as determined by the mean phycoerythrin fluorescence intensity. These data agree with our previous findings using metabolic labeling with ^{32}P and Western blotting with a P-Ser antibody, which show that only the wild-type galectin-3 transfectants undergo phosphorylation *in vivo* (7, 26, 27).

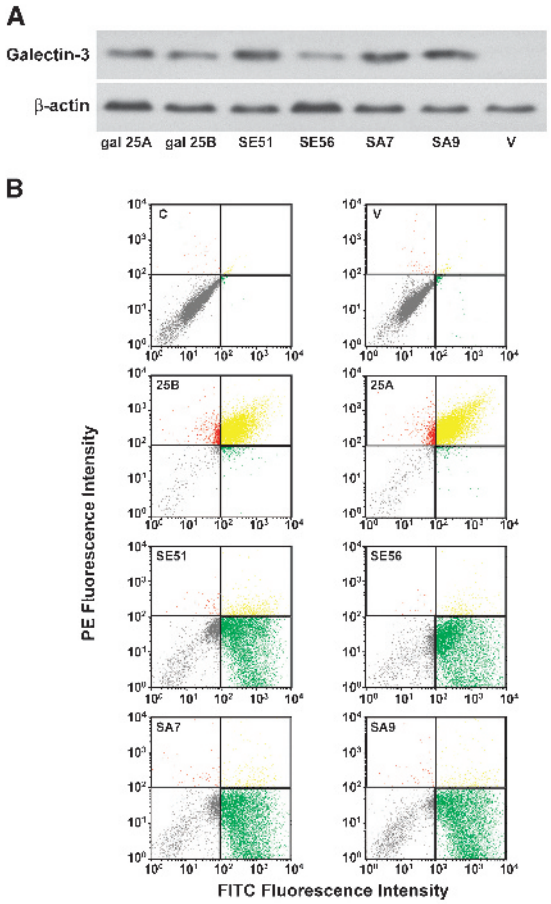

Cell Line	% FITC Positive	Mean FITC Fluorescence Intensity	% PE Positive	Mean PE Fluorescence Intensity
V	0	39.1	0.9	26.6
gal 25A	95.6	361.2	97.2	470.8
gal 25B	97.6	353.7	97.6	370.4
SE51	93.7	1008.2	1.5	33.3
SE56	95.4	252.0	2.4	24.5
SA7	93.3	979.6	2.9	23.3
SA9	90.7	994.3	2.4	22.7

Figure 1. Expression of galectin-3 and phospho-galectin-3 (Ser^6) in BT549 transfectant clones. *A,* Western blot detection of galectin-3 in total cell lysates of stable transfectants. BT549/V (*V*) represent control containing vehicle plasmid. BT549SA9 (*SA9*) and BT549SA7 (*SA7*) are phosphomutant (Ser^6→Ala) clones. BT549SE56 (*SE56*) and BT549SE51 (*SE51*) are phosphomutant (Ser^6-Glu) clones. BT549gal 25B (*gal 25B*) and BT549gal 25A (*gal 25A*) represent wild-type galectin-3-expressing clones. β-actin expression is shown as a loading control. *B,* flow cytometry. Two-dimensional dot plots of permeabilized BT549 transfectant clones (as in *A*) probed with anti-galectin-3 antibody (FITC fluorescence, *green*) and anti-phospho-galectin-3 (Ser^6) antibody [phycoerythrin (*PE*) fluorescence, *red*]. *Top left plot (C),* control isotype-matched IgG staining with both FITC and phycoerythrin-conjugated second antibodies. *Table,* percentage of the cell population of each clone that is positively stained with each antibody and the mean fluorescence intensity of each histogram.

Phosphorylation of galectin-3 is a prerequisite for malignant transformation. To investigate whether the phosphorylation status of galectin-3 correlates with tumorigenicity and malignant transformation, we explored the effect of phosphorylation status on tumor development in athymic nude mice. All mice (n = 10) injected with BT549gal 25A and BT549gal 25B cells (containing wild-type phosphorylated galectin-3) developed progressively growing tumors (Fig. 2*A*). In contrast, all mice (n = 25) injected with BT549 phosphomutant clones or BT549/V cells remained

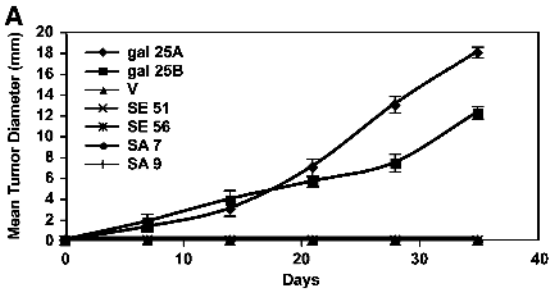

Spontaneous Lung Micrometastasis

Cells Inoculated	No. Mice	Weeks after Injection	No. Mice w/ Metastasis	No. Colonies in each Mouse
V	5	5	0	0
gal 25A	4	4	3	6, 1, 1
gal 25A	4	5	4	38, 10, 35, 8
gal 25B	5	5	5	14, 12, 10, 6, 15
SE51	5	5	0	0
SE56	5	5	0	0
SA 7	5	5	0	0
SA 9	5	5	0	0

Figure 2. Phosphorylation of galectin-3 is required for tumor growth and formation of pulmonary micrometastases in athymic mice. *A,* athymic nude mice were injected with 2×10^6 cells mixed in 0.1 mL of Matrigel into the mammary fat pad. Tumor diameters were measured weekly. Tumor grew in all mice injected with cells expressing wild-type galectin-3 but no tumors formed in the mice injected with cell expressing phosphomutant galectin-3 or vector alone. *B,* a colony of BT549gal 25A cells derived from the lungs of nude mice sacrificed 5 weeks after inoculation of BT549gal 25A cells in the fat pad. *Table,* spontaneous lung micrometastasis experiments showing the number of colonies formed in each mouse 4 to 5 weeks after injection with the different transfectants.

tumor-free for 40 days. In a separate experiment, the effect of galectin-3 phosphorylation status on spontaneous metastasis was examined. Autopsy did not reveal macroscopic metastases in the liver, lung, or lymph nodes of the tumor-bearing mice. However, three of four mice injected with BT549gal 25A developed lung micrometastases by 4 weeks after inoculation, with number of colonies ranging between one and six (Fig. 2*B*). When mice were sacrificed 5 weeks after inoculation, four of four and five of five mice injected with BT549gal 25Aand BT549gal 25B, respectively, showed lung micrometastases with higher numbers of colonies ranging from 8 to 38 for BT549gal 25A and 6 to 15 for BT549gal 25B (Fig. 2*B*). In contrast, none of the mice (0 of 20) injected with the phosphomutant galectin-3-expressing clones or with BT549/V control (0 of 5) developed lung micrometastasis (Fig. 2*B*). Tumorigenicity and metastasis of the galectin-3 transfectants correlated with the level of phospho-galectin-3 expression, but not with total galectin-3. The levels of total galectin-3 in gal 25A and gal 25B are similar as determined by Western blot and flow cytometry. The median FITC fluorescence intensity (total galectin-3) for gal 25A and gal 25B was 361.2 and 353.7, respectively. However, phospho-galectin-3 expression is 30% higher in gal 25A than in gal 25B (470.8 versus 370.4, median phycoerythrin fluorescence intensity; Fig. 1*B*). Tumors derived from BT549gal 25A had a significantly higher growth rate compared with BT549gal 25B tumors ($P < 0.0005$; Fig. 2*A*) and more aggressive metastatic behavior. The mean number of lung micrometastases colonies derived from gal 25A was 23 compared with 8.5 for gal 25B.

Effect of phospho-galectin-3 on cell cycle progression and proliferation. Cell-cycle progression analysis done by flow cytometry showed that stable expression of wild-type galectin-3 in BT549 cells resulted in a significant accumulation in G_2-M phase of the cell cycle compared with vector control (Fig. 3*A*). The number of cells in G_2-M phase was increased from 18.8% in BT549V to 27% and 24.1% in BT549gal 2A and gal 2B, respectively, and

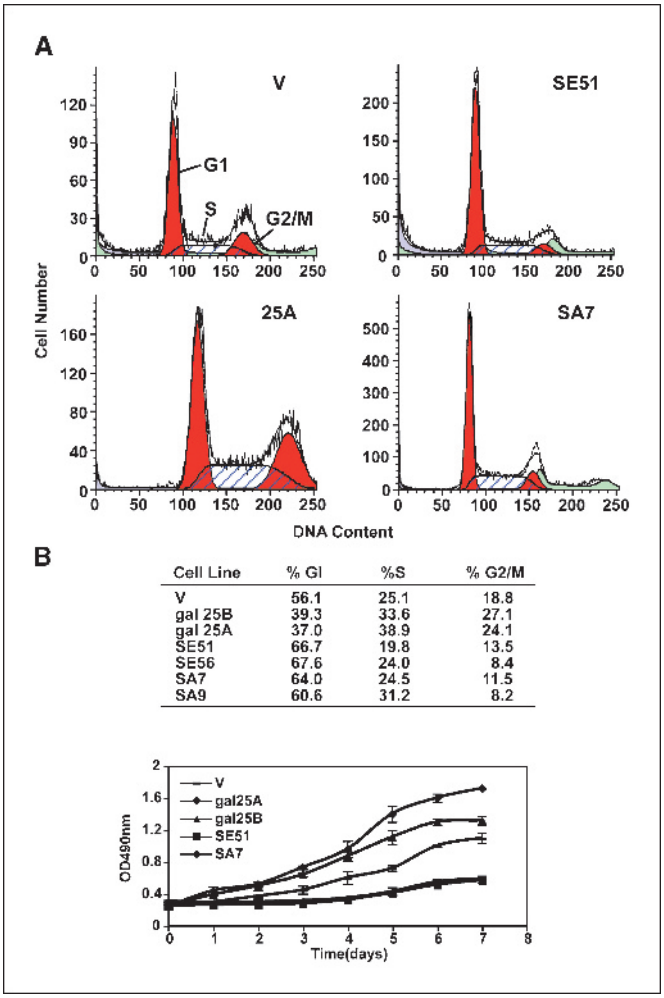

Figure 3. Phospho-galectin-3 induces a shift into G_2-M cell cycle phase and promotes growth *in vitro*. *A,* flow cytometric cell cycle histograms of BT549/V, BT549SE51, BT549gal 25A (*25A*), and BT549SA7. *Table,* proportions of cells in each cell cycle phase. *B, in vitro* cell growth of BT549 transfectants monitored by the MTS assay. Experiments were done with five transfectant clones in triplicates. BT549V control, BT549gal 25A, and BT549gal 25B are clones expressing wild-type galectin-3. BT549SE51 and BT549SA7 are transfectants expressing phosphomutant galectin-3: $Ser^6 \rightarrow$ Glu and $Ser^6 \rightarrow$ Ala, respectively.

Table 1. Differentially expressed genes found in both BT549ga1 25 A and BT549SE51

Genbank accession no.	Description	Symbol	Fold change		Gene ontology
			Wild type	Mutant	
NM_002982	*Small inducible cytokine A2*	CCL2	11.05	4.98	Immune response
NM_004114	*Fibroblast growth factor 13*	FGF13	10.55	11.02	Signal transduction
NM_000623	*Bradykinin receptor B2*	BDKRB2	3.84	5.57	Chemotaxis
U35622	*EWS protein/E1A enhancer binding protein chimera*	ETV4	3.78	4.51	Enhancer binding
NM_002160	*Hexabrachion*	TNC	3.49	8.04	Cell adhesion
NM_006404	*Protein C receptor, endothelial*	PROCR	3.43	6.15	Inflammatory response
NM_016357	*Epithelial protein lost in neoplasm β*	EPLIN	2.50	9.71	Transcription regulation from Pol II
NM_005384	*Nuclear factor, interleukin 3 regulated*	NFIL3	0.37	0.14	Immune response
NM_014868	*Ring finger protein 10*	RNF10	0.32	0.18	Cell growth and/or maintenance
NM_018459	*Uncharacterized bone marrow protein BM045*	BM045	0.29	0.31	Immune response
NM_001343	*Disabled homologue2*	DAB2	0.25	0.17	Cell proliferation
NM_004199	*Procollagen-proline, 2-oxoglutarate, 4-dioxygenase αpolypeptide II*	P4HA2	0.24	0.35	Protein proline hydroxylation
NM_006307	*Sushi-repeat-containing, protein X chromosome*	SRPX	0.24	0.12	Complement activation
NM_006622	*Serum-inducible kinase*	SNK	0.21	0.15	Protein phosphorylation
NM_003516	*H2A histone family, member O*	HIST2H2AA	0.20	0.23	Nucleosome assembly

decreased significantly in the phosphomutant clones (range 8.2-13.5%, $P < 0.005$). A concomitant decrease in the number of cells in G_1 from 56.1% of BT549V to 37.0% for BT549gal 25A and 39.3% for BT549gal 25B ($P < 0.005$ and $P < 0.002$, respectively) and a G_1 arrest for the phosphomutant clones were also observed (range 60.6-67.6%; Fig. 3*A*, *table*). Accordingly, enhanced growth rates were observed for BT549gal 25A and gal 25B relative to BT549V control ($P < 0.003$) as shown in Fig. 3*B*. Interestingly, the phosphomutant clones were significantly growth inhibited over the 8-day growth period compared with vector controls ($P < 0.003$; Fig. 3*B*). These results suggest a dominant negative activity for phosphomutant galectin-3. The transition from G_1 to G_2-M phase and enhanced proliferation observed in BT549gal 25A and gal 25B was not correlated with the expression of total galectin-3 but rather with the levels of phospho-galectin-3.

Identification of genes differentially expressed in cells containing phosphorylated and unphosphorylated galectin-3. To identify genes and pathways that may be regulated (directly or indirectly) by phospho-galectin-3, we did global differential gene expression analysis between BT549/gal 25A (contain wild-type galectin-3) and BT549/V control cells, and between BT549SE51 (contain phosphomutant galectin-3) and BT549/V cells. We identified 210 genes that were differentially expressed in BT549gal 25A relative to BT549V control using a 2.5-fold change as the cutoff. Of these genes, 22 were common to both BT549gal 25A and BT549SE51 (Table 1). Among the 188 genes that were unique to BT549/gal 25A (not differentially expressed in cells containing the phosphomutant galectin-3), 73 were highly up-regulated and 115 were significantly down-regulated. (A partial list is shown in Table 2 and the complete list is given in Supplementary Table S2) Of the 73 up-regulated genes, 17 either encode hypothetical proteins or have currently unknown functions. Among the 115 genes that were down-regulated in BT549/gal 25A, 25 encode hypothetical proteins or have unknown functions. *Glutathione S-transferase* and *retinoblastoma 1* were selected as strong feature genes supporting previously reported findings (17, 30). Glutathione is an important cofactor for the enzymatic decomposition of intracellular peroxidases by the glutathione peroxidase enzyme (31). Glutathione *S*-transferase was up-regulated >17-fold in BT549gal 25A, suggesting that overexpression of phospho-galectin-3 could cause a shift in oxidative metabolism, resulting in an increased demand for glutathione synthesis and a more oxidizing intracellular environment. Another antioxidant protein that was also up-regulated is the reversion-induced LIM protein.

Some of the genes identified in our screen have previously been associated with transformation and proliferation in breast and other tissues, whereas others represent novel markers of phospho-galectin-3 function. Examples of known differentially regulated genes include cyclin D1, retinoblastoma 1, and extracellular matrix proteins. Cyclin D_1 regulates the progression of the early to mid-G_1 phase of the cell cycle and is strongly implicated in breast tumorigenesis (32), in part explaining some of the growth-promoting and oncogenic action of phospho-galectin-3. Reorganization of the extracellular matrix proteins is an essential step for migration and invasion. Members of the keratin family are associated with metastasis in non–small cell lung cancer (33) and collagen has been reported to inhibit cell motility and migration (34). We have shown up-regulation of keratins 18 and 19, as well as down-regulation of several collagen genes, *IIIα1, Vα2*, and *IVα1* and *integrin α10* and *integrin α6*. Among the newly identified up-regulated genes involved in cell cycle regulation are those encoding cyclin B_2, serum deprivation response protein, and epiregulin. Novel down-regulated genes include fibroblast growth factor 2 and midkine.

The most highly expressed up regulated genes, not previously reported to be associated with breast carcinoma, were C-type lectin member 2 (CLECSF2), an activation-induced Ca^{2+}-dependent carbohydrate-binding integral membrane protein expressed in various cell types of hematopoietic origin (35); DUSP6, which blocks both the phosphorylation and enzymatic activity of the mitogen-activated protein kinase (MAPK) extracellular signal-regulated kinase (ERK; ref. 36); and two trypsinogens (PRSS3 and PRSS1). Serine protease trypsin and its precursor trypsinogen have been linked to tumor progression by activation of the matrix metalloproteinases in pancreatic, gastric, or colorectal cancer (37).

Among the most significantly down-regulated group of genes in BT549gal 25A were members of the cathepsin family (*L2, F, H, L-like 1*, and *L-like 3*). Cathepsins are papain family cysteine proteases that are a major component of the lysosomal proteolytic system. Recently, a novel noncaspase lysosomal apoptotic pathway in which the execution of apoptosis relies solely on the activation of cathepsins has been documented (38). Thus, our data suggest a potential protective role for phospho-galectin-3 in this newly discovered noncaspase apoptotic pathway.

Confirmation of microarray data by real-time quantitative reverse transcription-PCR and Western analysis. Real-time quantitative RT-PCR analysis of BT549gal 25A, BT549SE51, and BT549/V RNA was done to confirm the relative levels of expression in the transfectant clones for a subset of differentially expressed genes generated from the oligonucleotide microarray experiments. All (12 of 12) genes analyzed showed a pattern of transcript abundance consistent with the microarray data (Table 3).

The expression of selected proteins in BT549gal 25A, BT549SE51, and BT549/V was also compared by Western blotting. As shown in Fig. 4, the expression of IGBP5, PR553, DUSP6, cyclin D_1, and MUC5AC was up-regulated in BT549gal 25A cells but not in BT549SE51 or BT549/V cells. In contrast, CTSL2 and MUC1 expression was down-regulated in BT549gal 25A (data is shown for one representative clone of each transfectant group). These results agree well with the microarray predictions and the RT-PCR data and further confirm the reliability of the microarray analysis.

To evaluate the clinical relevance of genes predicted to be associated with phospho-galectin-3, we compared their expression in matched pairs of galectin-3 positive and negative breast tumor groups ($n = 10$). As a representative example, the relative quantity of four transcripts in the two tumor groups is shown in Fig. 5. CLECSF2 and IGFBP5 were up-regulated in all galectin-3-positive tumors, but not in galectin-3-negative tumors with a median of 3.3 $\pm$ 0.4 and 8.8 $\pm$ 0.9 fold increase, respectively ($P < 0.05$). Cyclin D_1 was up-regulated and cathepsins L2 was down-regulated in both groups, which is in accordance with the pattern observed in BT549gal25A.

Discussion

We report here that phosphorylation of galectin-3 is associated with alterations in expression of unique sets of genes and is a prerequisite for the tumorigenicity of human breast epithelial cells. We confirmed that overexpression of wild-type galectin-3 in human breast epithelial cells promotes tumorigenicity in athymic mice and development of spontaneous metastasis in the lung. These data is in accordance with previously published reports and support the hypothesis that nuclear galectin-3 is associated with tumor invasion and metastasis of breast cancer cells (39–41). Parallel experiments in which a mutant form of galectin-3 incapable of phosphorylation was introduced into galectin-3 null cells strongly suggest that phosphorylation of galectin-3 is necessary for tumor formation. Microarray analysis comparing transfectants expressing wild-type galectin-3 and those expression phosphomutant galectin-3 yielded further evidence that wild-type phosphorylated galectin-3 is associated with expression of a variety of key genes in several functional categories. This is further supported by additional data using RT-PCR and Western analysis to confirm microarray findings.

Table 2. Partial list of differentially expressed genes in BT549gal 25A but not BT549SE51

Genbank accession no.	Description	Symbol	Fold change	Gene ontology
NM_020300	*Microsomal glutathione S-transferase 1*	MGST1	17.65	Prostaglandin metabolism
NM_005127	*C-type lectin, superfamily member 2*	CLECSF2	15.22	Lectin
NM_002446	*MAPK kinase kinase 10*	MAP3K10	14.39	Signal transduction
NM_000224	*Keratin 18*	KRT18	13.61	Cytoskeleton organization
NM_000321	*Retinoblastoma 1*	RB1	12.93	Cell cycle checkpoint
NM_001946	*Dual specificity phosphatase 6*	DUSP6	11.52	Protein dephosphorylation
NM_002224	*Inositol 1,4,5-triphosphate receptor, 3*	ITPR3	11.43	Signal transduction
NM_002771	*Protease, serine, 3*	PRSS3	10.57	Proteolysis and peptidolysis
NM_002276	*Keratin 19*	KRT19	7.88	Cytoskeleton organization
NM_016445	*Pleckstrin 2 homologue*	PLEK2	7.40	Calcium binding
AF055033	*Insulin-like growth factor binding protein 5*	IGFBP5	6.65	Signal transduction
NM_002769	*Protease, serine, 1*	PRSS1	6.20	Proteolysis and peptidolysis
AF043909	*Gastric mucin*	MUC5AC	4.85	Cell adhesion
NM_004701	*Cyclin B2*	CCNB2	4.34	Cell cycle control
NM_002744	*Protein kinase C, ζ*	PRKCZ	3.58	Protein phosphorylation
NM_002755	*MAPK kinase 1*	MAP2K1	3.13	Signal transduction
NM_001758	*Cyclin D1*	CCND1	3.11	Cell cycle control
NM_000090	*Collagen, type III, α1*	COL3A1	0.03	Cell adhesion
NM_001333	*Cathepsin L2*	CTSL2	0.06	Proteolysis and peptidolysis
NM_000393	*Collagen, type V, α2*	COL5A2	0.08	Cell adhesion
NM_003637	*Integrin, α10*	ITGA10	0.10	Cell-matrix adhesion
NM_001845	*Collagen, type IV, α1*	COL4A1	0.13	Cell adhesion
NM_003793	*Cathepsin F*	CTSF	0.15	Proteolysis and peptidolysis
NM_004390	*Cathepsin H*	CTSH	0.15	Proteolysis and peptidolysis
L25629	*Human cathepsin-L-like*	CTSLL3	0.15	Proteolysis and peptidolysis
L25628	*Human cathepsin-L-like*	CTSLL2	0.22	Proteolysis and peptidolysis
NM_002456	*Mucin 1, transmembrane*	MUC1	0.26	Cholesterol catabolism
NM_000210	*Integrin, α6*	ITGA6	0.29	Cell-matrix adhesion

Table 3. Validation of microarray data by real-time quantitative RT-PCR

Gene accession no.	Gene name	Gene abbreviation	Fold change		
			Real-time PCR		Microarray
			gal 25A vs vector	SE51 vs vector	Gal 25A vs vector
NM_005127	*C-type lectin superfamily member 2*	CLECSF2	5,227.31 (4,390.93-6,223.00)	4.81 (4.45-5.19)	15.22
NM_000224	*Keratin 1B*	KRT18	63.92 (54.61-74.82)	2.43 (1.97-2.99)	13.61
NM_002224	*Inositol 1, 4, 5-triphosphate receptor, type 3*	ITPR3	49.53 (40.70-60.28)	0.34 (0.19-0.59)	11.43
NM_001946	*Dual specificity phosphatase 6*	DUSP6	44.58 (40.21-49.43)	2.52 (2.19-2.91)	11.52
NM_002771	*Protease, serine 3*	PRSS3	Expressed in gal 25A but not in vector	No expression in SE51 or vector	10.57
AF055033	*Insulin-like growth factor binding protein 5*	IGFBP5	42.14 (39.16-45.12)	1.38 (0.86+1.90)	6.65
NM_002306	*Galectin 3*	LGALS3	18.03 (15.39-21.11)	16.92 (13.89-20.51)	N/A
NM_053056	*Cyclin D1*	CCND1	3.79 (3.40-4.22)	1.34 (1.13-1.58)	3.11
NM_000090	*Collagen, type III, α1*	COL3A1	0.000041 (0.000044-0-00010)	0.37 (0.79-0.95)	0.03
NM_005264	*GDNF family receptor α1*	GFRA1	0.00043 (0.00029-0.00044)	0.59 (0.55-0.64)	0.05
NM_003637	*Integrin, α10*	ITGA10	0.028 (0.024-0.033)	0.88 (0.79-0.99)	0.10
NM_001333	*Cathepsin L2*	CTSL2	0.056 (0.039-0.080)	1.20 (1.0-1.45)	0.06

To identify potential mechanisms for the oncogenic property of phospho-galectin-3, we classified the differentially regulated genes into six functional categories: those involved in oxidative stress, apoptosis, cell cycle, signal transduction and transcriptional activation, cytoskeleton remodeling, and cell adhesion. The activation of diverse pathways by phospho-galectin-3 may reflect the functional diversity of galectin-3.

A possible role for phospho-galectin-3 in growth stimulation and tumorigenicity is supported by the up-regulation of cyclin D1 and members of the MAPK family, such as MAP3K10 and MAP2K1, suggesting that the c-Jun-NH_2-kinase pathway is activated, which is in accordance with previous reports (26). Cyclin D1 is overexpressed in ~50% of all breast cancers and its role in tumor progression is well established (42). The functional significance of cyclin D1 in breast cancer has been shown by gene-targeted silencing experiments. Cyclin D1 knockout mice are resistant to breast cancers induced by the *neu* and *ras* oncogenes, but remain fully sensitive to tumor driven by c-MYC or Wnt-1 (42). Phospho-galectin-3 may induce the expression of cyclin D1 either directly by binding/stabilization of nuclear protein-DNA complex formation at the Sp1 and cAMP-responsive element sites of the cyclin D1 promoter (20) or indirectly by activating the Wnt signaling pathway through binding upstream molecules like β-catenin (43, 44). Other signal transduction genes that seem to be regulated by phospho-galectin-3 include protein kinase C (PKC) ζ, IP3 receptor, tumor necrosis factor superfamily member 15, IGFBP5, and vascular endothelial growth factor β, which is down-regulated 3-fold. Overexpression of the IP3 receptor may alter Ca^{2+} release from internal pools by the second messenger IP3, resulting in activation of Ca^{2+}-dependent signaling pathways, such as calmodulin and PKC (45). It is of interest that two PKC substrates, the pleckstrin 2 homologue and serum deprivation response proteins, were also up-regulated by wild-type phosphorylated galectin-3.

Several genes in the cytoskeletal reorganization and cell adhesion pathways are also regulated in BT549gal 25A, including keratins 18 and 19. Keratins constitute the major intermediate filaments in several simple epithelial tissues and their presence has been used extensively in the diagnosis of tumors of epithelial and nonepithelial origin. For example, keratin 18 is commonly associated with both well and poorly differentiated carcinoma cells (46). In addition, γ-filamin is an actin-binding protein that is up-regulated by phospho-galectin-3 and actin filaments are key molecules in the regulation of cell adhesion, spreading, and

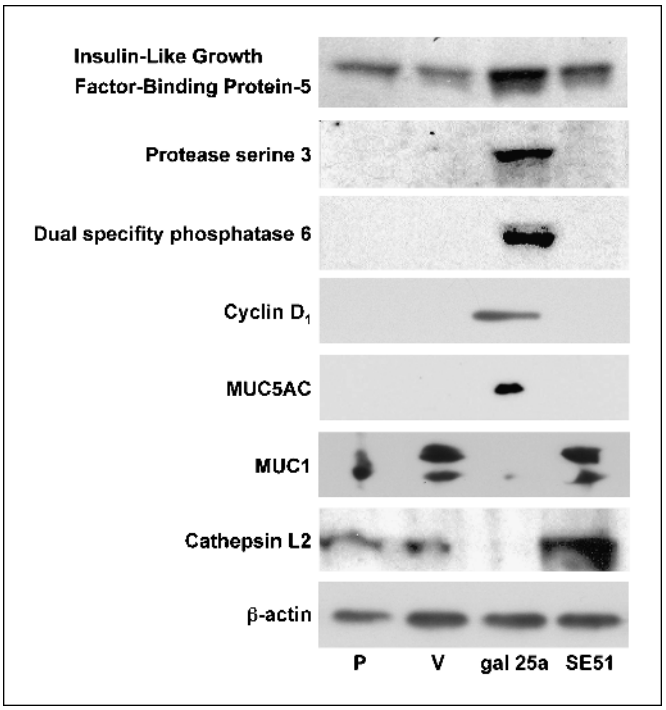

Figure 4. Protein expression profiles of a subset of differentially expressed genes from the microarray data in BT549 parental (*P*), BT549/V control, BT549gal95A, and BT549SE51.

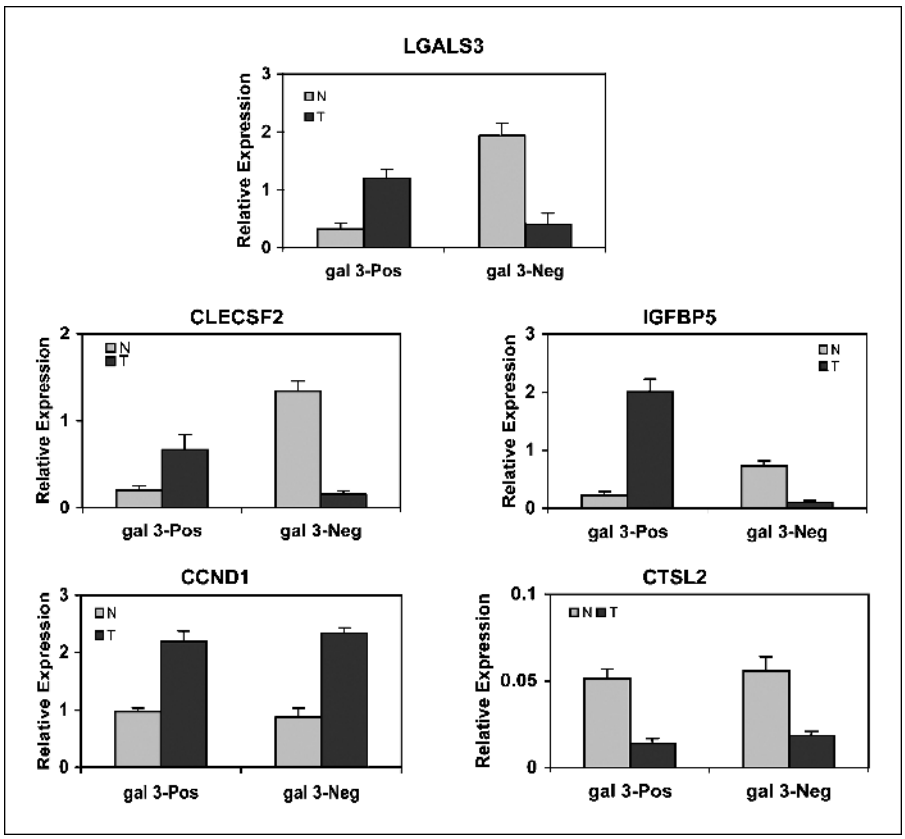

Figure 5. Real-time quantitative RT-PCR analysis of selected differentially expressed genes from microarray data in panel of matched pairs of galectin-3-positive (*gal 3-Pos*) and galectin-3-negative (*gal 3-Neg*) breast tumors.

configuration. *Integrin α10* and *integrin α6*, which are down-regulated, are regarded as invasion suppressor genes in many types of cancers (47). Suppressed expression of these genes in the transformed BT549gal 25A is in agreement with the metastatic potential of these cells. Among the genes most strongly down-regulated by phospho-galectin-3 are several collagen genes: *collagen III αI, collagen V α2*, and *collagen IV α1*.

It is of interest that phospho-galectin-3 suppressed expression of the transmembrane mucin MUC1 and up-regulated the secreted gel forming mucin MUC5AC. Mucins are large extracellular proteins that are heavily glycosylated with broad functions that include protection and lubrication. Altered expression of mucin gene products or their glycosylation pattern accompanies the development of cancer and influences adhesion and invasion (48). MUC1 is normally expressed ubiquitously on the ducts and glands of simple secretary epithelial tissues. Overexpression of MUC1 by breast cancers has been reported and correlates with poor survival (49). MUC5AC is highly expressed in the goblet cells of the human airway and gastric epithelium and is a tumor-associated marker in the colon (48). The cytoplasmic moiety of MUC1 participates in intracellular signaling by interacting with the erb B receptors resulting in epidermal growth factor–dependent activation of RAS and ERK 1/2 MAPK pathway. The extracellular portion of MUC1, like MUC5AC, interacts with ICM-1 on endothelium, aiding in the metastatic spread of tumor cells (49). Our observation that MUC1 is replaced by MUC5AC in the model system we used requires further study to determine its functional significance. A functional link between mucins, galectin-3, and metastasis has been shown in our laboratory. Silencing of galectin-3 in highly metastatic human cancer cells resulted in reduced expression of MUC2 and inhibition of tumor growth and liver metastases in athymic mice (16).

IGFBP5 and CLECSF2 were found to be up-regulated in both BT549gal 25A, BT549gal 25B, and in galectin-3-positive breast tumors. The IGFBPs are a family of proteins that bind with high affinity to insulin growth factors and modulate their mitogenic actions by regulating their ability to interact with their signaling receptor (50). The role of IGFBP5 in human breast cancer cell growth is complex, with some reports that it may be growth inhibitory and associated with induction of apoptosis, whereas others show a survival role in response to apoptotic stimuli (51). CLECSF2 is an integral membrane protein that recognizes carbohydrate chains in a Ca^{2+}-dependent manner and is involved in host defense mechanisms (35). It can trigger protein tyrosine phosphorylation pathways, thus providing an alternative route to growth hormones signaling C-type lectin, which is expressed preferentially in lymphoid tissues and in most hematopoietic cell types (52). Transcription of CLECSF2 was transiently up-regulated during lymphocyte activation by phorbol ester. A functional role for CLECSF2 is breast cancer remains to be established.

The series of experiments described in this paper provide evidence that sustained phosphorylation of galectin-3 is associated with the tumorigenic potential of human breast epithelial cells. The data show the functional diversity of galectin-3 and suggest that phosphorylation of the protein is necessary for regulation of genes in a variety of functional categories that may play a role in malignant transformation.

Acknowledgments

Received 9/14/2004; revised 9/9/2005; accepted 9/21/2005.

Grant support: NIH/National Cancer Institute grants CA 69480 (R.S. Bresalier), CA 46120 (A. Raz), and Cancer Center Support grant CA 16672 (J.E. Price).

The costs of publication of this article were defrayed in part by the payment of page charges. This article must therefore be hereby marked *advertisement* in accordance with 18 U.S.C. Section 1734 solely to indicate this fact.

We thank Drs. L. Hu, K. Coomes, V.R. Dunmire, and D.E. Cogdell for performing and analyzing the microarray and real-time RT-PCR experiments and R. Pickens for preparation of the manuscript.

References

1. Barondes SH, Castronovo V, Cooper DN, et al. Galectins: a family of animal β-galactoside-binding lectins. Cell 1994;76:597–8.
2. Hsu DK, Liu FT. Regulation of cellular homeostasis by galectins. Glycoconj J 2004;19:507–15.
3. Leffler H, Carlsson S, Hedlund M, Qian Y, Poirier F. Introduction to galectins. Glycoconj J 2004;19:433–40.
4. Abbott WM, Hounsell EF, Feizi T. Further studies of oligosaccharide recognition by the soluble 13 kDa lectin of bovine heart muscle. Ability to accommodate the blood-group-H and -B-related sequences. Biochem J 1988;252:283–7.
5. Hirabayashi J, Kasai K. The family of metazoan metal-independent β-galactoside-binding lectins: structure, function and molecular evolution. Glycobiology 1993;3:297–304.
6. Kadrofske MM, Openo KP, Wang JL. The human LGALS3 (galectin-3) gene: determination of the gene structure and functional characterization of the promoter. Arch Biochem Biophys 1998;349:7–20.
7. Gong HC, Honjo Y, Nangia-Makker P, et al. The NH_2 terminus of galectin-3 governs cellular compartmentalization and functions in cancer cells. Cancer Res 1999;59:6239–45.
8. Ochieng J, Furtak V, Lukyanov P. Extracellular functions of galectin-3. Glycoconj J 2004;19:527–35.
9. Yang RY, Hsu DK, Liu FT. Expression of galectin-3 modulates T-cell growth and apoptosis. Proc Natl Acad Sci U S A 1996;93:6737–42.
10. Akahani S, Nangia-Makker P, Inohara H, Kim HR, Raz A. Galectin-3: a novel antiapoptotic molecule with a functional BH1 (NWGR) domain of Bcl-2 family. Cancer Res 1997;57:5272–6.
11. Matarrese P, Tinari N, Semeraro ML, Natoli C, Iacobelli S, Malorni W. Galectin-3 overexpression protects from cell damage and death by influencing mitochondrial homeostasis. FEBS Lett 2000;473:311–5.
12. Takenaka Y, Fukumori T, Raz A. Galectin-3 and metastasis. Glycoconj J 2004;19:543–9.
13. van den Brule F, Califice S, Castronovo V. Expression of galectins in cancer: a critical review. Glycoconj J 2004;19:537–42.
14. Lahm H, Andre S, Hoeflich A, et al. Tumor galectinology: insights into the complex network of a family of endogenous lectins. Glycoconj J 2004;20:227–38.
15. Grassadonia A, Tinari N, Iurisci I, et al. 90K (Mac-2 BP) and galectins in tumor progression and metastasis. Glycoconj J 2004;19:551–6.
16. Bresalier RS, Mazurek N, Sternberg LR, et al. Metastasis of human colon cancer is altered by modifying expression of the β-galactoside-binding protein galectin 3. Gastroenterology 1998;115:287–96.
17. Takenaka Y, Inohara H, Yoshii T, et al. Malignant transformation of thyroid follicular cells by galectin-3. Cancer Lett 2003;195:111–9.
18. Nangia-Makker P, Thompson E, Ochieng J, Raz A. Induction of tumorigenicity by galectin-3 in a non-tumorigenic human breast carcinoma cell line. Int J Oncol 1995;7:1079–87.
19. Patterson RJ, Wang W, Wang JL. Understanding the biochemical activities of galectin-1 and galectin-3 in the nucleus. Glycoconj J 2004;19:499–506.
20. Lin HM, Pestell R, Raz A, Kim HR. Galectin-3 enhances cyclin D1 promoter activity through SP1 and a cAMP-responsive element in human breast epithelial cells. Oncogene 2002;21:8001–10.
21. Dudas SP, Yunker CK, Sternberg LR, Byrd JC, Bresalier RS. Expression of human intestinal mucin is modulated by the β-galactoside binding protein galectin-3 in colon cancer. Gastroenterology 2002;123:817–26.
22. Walzel H, Blach M, Hirabayashi J, Arata Y, Kasai K, Brock J. Galectin-induced activation of the transcription factors NFAT and AP-1 in human Jurkat T-lymphocytes. Cell Signal 2002;14:861–8.
23. Paron I, Scaloni A, Pines A, et al. Nuclear localization of galectin-3 in transformed thyroid cells: a role in transcriptional regulation. Biochem Biophys Res Commun 2003;302:545–53.
24. Huflejt ME, Turck CW, Lindstedt R, Barondes SH, Leffler H. L-29, a soluble lactose-binding lectin, is phosphorylated on serine 6 and serine 12 *in vivo* and by casein kinase I. J Biol Chem 1993;268:26712–8.
25. Mazurek N, Conklin J, Byrd JC, Raz A, Bresalier RS. Phosphorylation of the β-galactoside-binding protein galectin-3 modulates binding to its ligands. J Biol Chem 2000;275:36311–5.
26. Takenaka Y, Fukumori T, Yoshii T, et al. Nuclear export of phosphorylated galectin-3 regulates its anti-apoptotic activity in response to chemotherapeutic drugs. Mol Cell Biol 2004;24:4395–406.
27. Yoshii T, Fukumori T, Honjo Y, Inohara H, Kim HR, Raz A. Galectin-3 phosphorylation is required for its anti-apoptotic function and cell cycle arrest. J Biol Chem 2002;277:6852–7.
28. Price J, Polyzos A, Zhang R, Daniels L. Tumorigenicity and metastasis of human breast carcinoma cell lines in nude mice. Cancer Res 1990;50:17–21.
29. Yang Y, Dudoit S, Luu P, et al. Normalization for cDNA microarray data: a robust composite method addressing single and multiple slide systematic variation. Nucleic Acids Res 2002;30:e15.
30. Lee Y, Song Y, Song J, et al. Reconstitution of galectin-3 alters glutathione content and potentiates TRAIL-induced cytotoxicity by dephosphorylation of Akt. Exp Cell Res 2003;288:21–34.
31. Scott E, Wright R. Variability of glutathione *S*-transferase of human erythrocytes. Am J Hum Genet 1980;32:115–7.
32. Hinds PW, Dowdy SF, Eaton EN, Arnold A, Weinberg RA. Function of a human cyclin gene as an oncogene. Proc Natl Acad Sci U S A 1994;91:709–13.
33. Ueda Y, Fujita J, Bandoh S, et al. Expression of cytokeratin 19 mRNA in human lung cancer cell lines. Int J Cancer 1999;81:939–43.
34. Erdel M, Spiess E, Trefz G, Boxberger HJ, Ebert W. Cell interactions and motility in human lung tumor cell lines HS-24 and SB-3 under the influence of extracellular matrix components and proteinase inhibitors. Anticancer Res 1992;12:349–59.
35. Hamann J, Montgomery KT, Lau S, Kucherlapati R, van Lier RA. AICL: a new activation-induced antigen encoded by the human NK gene complex. Immunogenetics 1997;45:295–300.
36. Camps M, Nichols A, Arkinstall S. Dual specificity phosphatases: a gene family for control of MAP kinase function. FASEB J 2000;14:6–16.
37. Yamamoto H, Iku S, Adachi Y, et al. Association of trypsin expression with tumour progression and matrilysin expression in human colorectal cancer. J Pathol 2003;199:176–84.
38. Cirman T, Oresic K, Mazovec GD, et al. Selective disruption of lysosomes in HeLa cells triggers apoptosis mediated by cleavage of Bid by multiple papain-like lysosomal cathepsins. J Biol Chem 2004;279:3578–87.
39. Moon B, Lee Y, Battle P, Jessup J, Raz A, Kim H. Galectin-3 protects human breast carcinoma cells against nitric oxide-induced apoptosis: implication of galectin-3 function during metastasis. Am J Pathol 2001;159:1055–60.
40. Song YK, Billiar TR, Lee YJ. Role of galectin-3 in breast cancer metastasis: involvement of nitric oxide. Am J Pathol 2002;160:1069–75.
41. John CM, Leffler H, Kahl-Knutsson B, Svensson I, Jarvis GA. Truncated galectin-3 inhibits tumor growth and metastasis in orthotopic nude mouse model of human breast cancer. Clin Cancer Res 2003;9:2374–83.
42. Yu Q, Geng Y, Sicinski P. Specific protection against breast cancers by cyclin D1 ablation. Nature 2001;411:1017–21.
43. Shimura T, Takenaka Y, Tsutsumi S, Hogan V, Kikuchi A, Raz A. Galectin-3, a novel binding partner of β-catenin. Cancer Res 2004;64:6363–7.
44. Shimura T, Takenaka Y, Fukumori T, et al. Implication of galectin-3 in Wnt signaling. Cancer Res 2005;65:3535–7.
45. Maranto AR. Primary structure, ligand binding, and localization of the human type 3 inositol 1,4,5-trisphosphate receptor expressed in intestinal epithelium. J Biol Chem 1994;269:1222–30.
46. Chu PG, Weiss LM. Keratin expression in human tissues and neoplasms. Histopathology 2002;40:403–39.
47. Parise LV, Lee J, Juliano RL. New aspects of integrin signaling in cancer. Semin Cancer Biol 2000;10:407–14.
48. Byrd JC, Bresalier RS. Mucins and mucin binding proteins in colorectal cancer. Cancer Metastasis Rev 2004;23:77–99.
49. Gendler SJ. MUC1, the renaissance molecule. J Mammary Gland Biol Neoplasia 2001;6:339–53.
50. Jones JI, Clemmons DR. Insulin-like growth factors and their binding proteins: biological actions. Endocr Rev 1995;16:3–34.
51. Butt AJ, Dickson KA, McDougall F, Baxter RC. Insulin-like growth factor-binding protein-5 inhibits the growth of human breast cancer cells *in vitro* and *in vivo*. J Biol Chem 2003;278:29676–85.
52. Eichler W, Ruschpler P, Wobus M, Drossler K. Differentially induced expression of C-type lectins in activated lymphocytes. J Cell Biochem 2001;81:201–8.

Phosphorylation of Galectin-3 Contributes to Malignant Transformation of Human Epithelial Cells via Modulation of Unique Sets of Genes

Nachman Mazurek, Yun Jie Sun, Janet E. Price, et al.

Cancer Res 2005;65:10767-10775.